

Table V. Intramolecular Dimensions

Bond Lengths, Å			
Cu(1)-O(1)	1.876 (7)	Cu(2)-O(3)	1.857 (7)
Cu(1)-O(2)	1.866 (7)	Cu(2)-O(4)	1.858 (9)
Cu(1)-N(1)	2.015 (8)	Cu(2)-N(3)	1.997 (8)
Cu(1)-N(2)	2.030 (8)	Cu(2)-N(4)	2.012 (9)
N(1)-C(1)	1.28 (1)	N(3)-C(18)	1.27 (1)
C(1)-C(2)	1.47 (1)	C(18)-C(19)	1.51 (2)
C(1)-C(3)	1.49 (1)	C(18)-C(20)	1.50 (2)
C(3)-C(4)	1.55 (1)	C(20)-C(21)	1.51 (2)
C(4)-O(1)	1.35 (1)	C(21)-C(22)	1.58 (2)
C(4)-C(5)	1.54 (1)	C(21)-C(23)	1.49 (2)
C(4)-C(6)	1.53 (2)	C(21)-O(3)	1.34 (1)
N(2)-C(7)	1.27 (1)	N(4)-C(24)	1.25 (2)
C(7)-C(8)	1.52 (2)	C(24)-C(25)	1.58 (2)
C(7)-C(9)	1.47 (1)	C(24)-C(26)	1.57 (2)
C(9)-C(10)	1.50 (1)	C(26)-C(27)	1.46 (2)
C(10)-C(11)	1.55 (2)	C(27)-C(28)	1.54 (2)
C(10)-C(12)	1.57 (2)	C(27)-C(29)	1.56 (2)
C(10)-O(2)	1.38 (1)	C(27)-O(4)	1.35 (1)
N(1)-C(13)	1.46 (1)	N(4)-C(31)	1.40 (1)
C(13)-C(14)	1.49 (1)	C(31)-C(32)	1.52 (2)
C(14)-C(15)	1.51 (1)	C(32)-C(33)	1.52 (1)
C(15)-C(16)	1.51 (1)	C(33)-C(34)	1.51 (1)
C(16)-C(30)	1.59 (1)	C(34)-C(17)	1.51 (1)
C(30)-N(3)	1.45 (1)	C(17)-N(2)	1.44 (1)
mean C-F	1.32 (1)	mean C-F	1.34 (2)
Bond Angles, Deg			
O(1)-Cu(1)-O(2)	161.0 (3)	O(3)-Cu(2)-O(4)	172.9 (4)
N(1)-Cu(1)-N(2)	156.6 (3)	N(3)-Cu(2)-N(4)	164.8 (4)
O(1)-Cu(1)-N(1)	92.7 (3)	O(3)-Cu(2)-N(3)	91.4 (3)
N(1)-Cu(1)-O(2)	88.8 (3)	N(3)-Cu(2)-O(4)	87.8 (4)
O(2)-Cu(1)-N(2)	96.2 (3)	O(4)-Cu(2)-N(4)	92.9 (4)
N(2)-Cu(1)-O(1)	89.9 (3)	N(4)-Cu(2)-O(3)	89.7 (4)
Cu(1)-N(1)-C(1)	123.0 (7)	Cu(2)-N(3)-C(18)	121.8 (8)
Cu(1)-N(1)-C(13)	114.1 (6)	Cu(2)-N(3)-C(30)	116.1 (6)
C(13)-N(1)-C(1)	122.4 (8)	C(18)-N(3)-C(30)	121.7 (9)
N(1)-C(1)-C(2)	125.6 (9)	N(3)-C(18)-C(19)	125 (1)
N(1)-C(1)-C(3)	118.1 (9)	N(3)-C(18)-C(20)	117 (1)
C(2)-C(1)-C(3)	116.2 (9)	C(19)-C(18)-C(20)	118 (1)
C(1)-C(3)-C(4)	115.0 (8)	C(18)-C(20)-C(21)	117 (1)
C(3)-C(4)-O(1)	114.7 (8)	C(20)-C(21)-O(3)	115 (1)
C(3)-C(4)-C(5)	106.1 (8)	C(20)-C(21)-C(22)	107 (1)
O(1)-C(4)-C(5)	108.1 (8)	C(20)-C(21)-C(23)	109 (1)
C(3)-C(4)-C(6)	110.1 (9)	C(22)-C(21)-C(23)	108 (2)
C(5)-C(4)-C(6)	107.6 (9)	C(22)-C(21)-O(3)	109 (1)
C(6)-C(4)-O(1)	110.0 (9)	C(23)-C(21)-O(3)	109 (1)
C(4)-O(1)-Cu(1)	125.6 (6)	C(21)-O(3)-Cu(2)	124.4 (8)
Cu(1)-N(2)-C(7)	122.0 (7)	Cu(2)-N(4)-C(24)	120 (1)
Cu(1)-N(2)-C(17)	115.1 (6)	Cu(2)-N(4)-C(31)	117.8 (8)
C(17)-N(2)-C(7)	122.9 (9)	C(24)-N(4)-C(31)	122 (1)
N(2)-C(7)-C(8)	125 (1)	N(4)-C(24)-C(25)	123 (1)
N(2)-C(7)-C(9)	122 (1)	N(4)-C(24)-C(26)	119 (1)
C(8)-C(7)-C(9)	113 (1)	C(25)-C(24)-C(26)	118 (1)
C(7)-C(9)-C(10)	118 (1)	C(24)-C(26)-C(27)	117 (1)
C(9)-C(10)-O(2)	115 (1)	C(26)-C(27)-C(28)	112 (1)
C(9)-C(10)-C(11)	111 (1)	C(26)-C(27)-C(29)	110 (1)
C(9)-C(10)-C(12)	108 (1)	C(26)-C(27)-O(4)	114 (1)
C(11)-C(10)-O(2)	107 (1)	C(28)-C(27)-C(29)	105 (2)
C(11)-C(10)-C(12)	108 (1)	C(28)-C(27)-O(4)	107 (1)
C(12)-C(10)-O(2)	106 (1)	C(29)-C(27)-O(4)	109 (1)
C(10)-O(2)-Cu(1)	123.9 (7)	C(27)-O(4)-Cu(2)	126.2 (8)
N(1)-C(13)-C(14)	110.2 (8)	N(4)-C(31)-C(32)	113 (1)
C(13)-C(14)-C(15)	116.7 (9)	C(31)-C(32)-C(33)	115 (1)
C(14)-C(15)-C(16)	109.4 (8)	C(32)-C(33)-C(34)	112.9 (9)
C(15)-C(16)-C(30)	111.7 (9)	C(33)-C(34)-C(17)	116.6 (9)
C(16)-C(30)-N(3)	107.7 (8)	C(34)-C(17)-N(2)	114.5 (9)
Cu(1) mean F-C-F	107 (1)	Cu(2) mean F-C-F	108 (2)
Cu(1) mean C-C-F	112 (1)	Cu(2) mean C-C-F	110 (2)

five C atoms joining the imino nitrogen atoms of the ligands. The large ring structure so formed is 16-membered. The weighted mean C-C bond within the chains is 1.518 (5) Å, and the weighted mean C-C-C angle is 112.6 (3)°. Both values are indistinguishable from those of 1.512 (6) Å and 113.0 (3)° observed previously.² The trifluoromethyl groups attached to the chelate rings are undergoing considerable

thermal motion. Weighted mean dimensions for these groups are given in Table V.

Discussion

In our original report² of the preparation of this copper complex and its homologues with $n = 2-12$, we suggested that they were all mononuclear type 1 structures. This conclusion was based on solution measurements of molecular weight by vapor-pressure osmometry in acetonitrile solution (found, 581; calcd for $n = 5$, 576), but it is clear from the current result that the solution molecular weight is not a reliable guide to the degree of aggregation in the solid state for $n = 5$ and, in all probability, analogous copper complexes. In contrast, the nickel complex with $n = 6$ showed good agreement between the solution molecular weight and the dinuclear structure found in the crystal.²

There are two possible explanations for this effect. It could be that, in the original formation of the complex, the dinuclear and mononuclear structures were both formed but were fortuitously separated in the subsequent recrystallization procedure. Alternatively, there could be an equilibrium between a dinuclear structure in the crystal and a mononuclear structure in solution.

The first explanation may be rejected, since we have seen no evidence for the existence of two isomeric forms of any of the copper complexes in this study. Samples used for the molecular weight measurement and the crystallographic study had been treated in the same way, and accidental separation into mononuclear and dinuclear forms can be excluded.

The existence of an equilibrium between mononuclear and dinuclear forms is consistent with an observation made in our previous work: that the solution molecular weight is dependent on the choice of solvent. Good agreement with calculated values was found in a polar solvent (CH₃CN), but use of less polar solvents (CHCl₃, C₆H₆) gave higher values, suggesting some degree of aggregation. The tendency to form dinuclear units in the solid state is presumably favored by the trans geometry of N₂O₂ ligand atoms around the metal ion which this permits. It is interesting that the dinuclear unit changes in solution to the mononuclear unit (which would be entropy favored) for the Cu²⁺ complex but not for the less labile Ni²⁺. Further studies are being undertaken to investigate the generality of this effect.

Acknowledgment. We thank the National Sciences and Engineering Research Council of Canada for financial support for this work, through grants to N.C.P. and C.J.W.

Registry No. 2 (M = Cu, $n = 5$), 75067-38-8.

Supplementary Material Available: A listing of structure amplitudes, as $10|F_o|$ vs. $10|F_c|$ in electrons, weighted least-squares planes, and torsional angles for the six-membered rings (13 pages). Ordering information is given on any current masthead page.

Contribution from the Department of Inorganic Chemistry,
Indian Association for the Cultivation of Science,
Calcutta 700 032, India

Synthesis, Structure, and Electrochemistry of Dihalobis(α -benzil oximate)ruthenium(III)

A. R. Chakravarty and A. Chakravorty*

Received May 12, 1980

There is much current interest in the chemistry of ruthenium pertaining to the synthesis of new complexes, structure, reactivity and catalysis, intervalence phenomena, and phenomena related to electron transfer and energy transfer. We have

undertaken a project covering some of these areas, the first step being generation of new complexes. The synthesis, characterization, and electron-transfer behavior of haloruthenium complexes of α -benzil oxime, $C_6H_5C(=O)C(=NOH)C_6H_5$, are reported here. The ligand is abbreviated as HB. It is noted that ruthenium complexes of oxime ligands have not been studied much.¹

Experimental Section

Materials. Ruthenium trichloride was obtained from Arora-Matthey, Calcutta. It was converted to $RuCl_3 \cdot 3H_2O$ by repeated evaporation to dryness with concentrated hydrochloric acid. Lithium bromide of E. Merck make was used. Benzil (E. Merck) was converted to α -benzil oxime by using a standard method.² Tetraethylammonium bromide (Fluke AG) was converted³ to tetraethylammonium perchlorate (TEAP). Acetonitrile for electrochemical purposes was prepared by purifying the commercial solvent with CaH_2 treatment followed by distillation over P_2O_{10} . The voltage window at platinum was (+1.5 to -1.0 V vs. SCE) quite adequate for the present study. Solvents used for spectroscopy and other measurements were of analytical grade available commercially.

Physical Measurements. Spectroscopic data were obtained by using the following instruments: IR (KBr disk, 4000–400 cm^{-1}), Beckman IR-20A spectrophotometer; far-IR (polyethylene disk, 400–100 cm^{-1}), Beckman IR-720M spectrophotometer; electronic spectra, Cary 17D spectrophotometer; X-band EPR, JEOL-3X100 spectrometer. Magnetic susceptibility was measured in a Gouy balance with $CoHg(SCN)_4$ as standard. Solution electrical conductivity was measured by using a Philips PR9500 bridge. Electrochemical measurements were made with the help of a PAR Model 370-4 electrochemistry system. Cyclic voltammetry required the PAR 174A polarographic analyzer and PAR 175 universal programmer and a PAR RE 0074 XY recorder. The three electrode measurements were carried out by using a planar Beckman Model 39273 platinum-inlay working electrode, a platinum-wire auxiliary electrode, and a saturated calomel reference electrode (SCE). The results reported are uncorrected for junction potentials. Controlled potential coulometry was performed by using a PAR 173 potentiostat, PAR 179 digital coulometer, and PAR 377A cell system taken in conjunction with a platinum-wire-gauge working electrode.

Preparation of Complexes. Dichlorobis(α -benzil oximato)ruthenium(III), $RuCl_2(HB)(B)$. A total of 0.45 g (2 mmol) of HB was added to a stirred solution of 0.26 g (1 mmol) of $RuCl_3 \cdot 3H_2O$ in 20 mL of absolute ethanol. The mixture was warmed to 50 °C, and stirring was continued for 2 h. It was then cooled to 0 °C, and the precipitated complex was collected by filtration and washed thoroughly with water and finally with ethanol. The brown crystals (red, when powdered) thus obtained were dried in vacuo over P_2O_{10} . Recrystallization was done from a dichloromethane-diethyl ether mixture. The yield was 0.3 g (~50%). Anal. Calcd for $RuC_{28}H_{21}N_2O_2Cl_2$: C, 54.09; H, 3.35; N, 4.51; Cl, 11.43. Found: C, 54.29; H, 3.52; N, 4.57; Cl, 11.60.

Dibromobis(α -benzil oximato)ruthenium(III), $RuBr_2(HB)(B)$. This was prepared by the same procedure except that the $RuCl_3 \cdot 3H_2O$ was stirred for 10 min with 1 g of LiBr in 20 mL of absolute ethanol prior to the addition of HB. The yield was 0.4 g (~57%). Anal. Calcd for $RuC_{28}H_{21}N_2O_2Br_2$: C, 47.33; H, 2.96; N, 3.94. Found: C, 47.41; H, 3.23; N, 3.83.

Results and Discussion

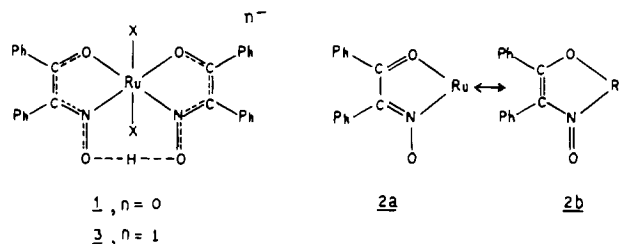
Synthesis and Structure. Hydrated RuX_3 ($X = Cl, Br$) smoothly reacts with HB giving crystalline complexes in which $Ru:ligand:X = 1:2:2$. Magnetic, spectroscopic, and electrochemical results unequivocally establish metal oxidation state as +3. The complexes are thus correctly formulated as $RuX_2(HB)(B)$. Some physical data are collected in Table I.

Table I. Physical Data for Complexes $RuX_2(HB)(B)$

physical quantity	$RuCl_2(HB)(B)$	$RuBr_2(HB)(B)$
Molar Conductivity ^a		
$\Lambda_M, \Omega^{-1} cm^{-1} M^{-1}$	13.0	24.0
Infrared Spectra ^b		
$\nu_{C=N} + \nu_{C=C}$	1590	1595
ν_{CO}	1530	1530
ν_{NO}	1290	1295
ν_{Ru-X}	358	299
Bulk Susceptibility ^c (298 K)		
μ_{eff}, μ_B	1.80	2.20
EPR Spectra (PC, ^d FB, ^e B ^f)		
g_{\parallel}	1.96, 1.93, ...	1.85, 1.83, ...
g_{\perp}	2.45, 2.46, ...	2.51, 2.54, ...
g_{av}	2.29, ^g 2.28, ^g 2.32	2.29, ^g 2.30, ^g 2.39
Electronic Spectra ^h		
λ, nm	544	522
$\epsilon, M^{-1} cm^{-1}$	9660	7000
λ, nm	648 ⁱ	635 ^j
$\epsilon, M^{-1} cm^{-1}$	16350 ⁱ	16150 ^j

^a In acetonitrile at 298 K. ^b In KBr disk (4000–400 cm^{-1}) and in polyethylene disk (400–100 cm^{-1}). ^c Gouy method using $CoHg(SCN)_4$ as standard. ^d Polycrystalline sample at 298 K. ^e Frozen benzene at 123 K. ^f In benzene at 298 K. ^g $g_{av} = (2g_{\perp} + g_{\parallel})/3$. ^h In acetonitrile at 298 K. ⁱ For $RuCl_2(HB)(B)^+$, a coulometrically reduced solution of **1**. ^j For $RuBr_2(HB)(B)^+$, a coulometrically reduced solution of **1**.

The presence of a *single*, sharp, and very strong ν_{Ru-X} frequency suggests a trans stereochemistry for the RuX_2 moiety as in **1**. In acetonitrile solution electrical conductivities are



small, indicating marginal dissociation of X^- in such solution. Presence of strong intramolecular hydrogen bonding in complexes is known to broaden and weaken stretching and bending vibrations of the $O \cdots H \cdots O$ moiety to the point where it may be difficult⁴ or even impossible⁵ to observe them. Our failure to locate such bands in the 1600–2500- cm^{-1} region in **1** is thus not too surprising. A strong and somewhat broad band at 1530 cm^{-1} (absent in HB) is assigned to ν_{CO} of the complex. The unusually low frequency is suggestive of the ring resonance $2a \leftrightarrow 2b$ probably assisted by metal participation. A similar effect is known to exist in the violuric acid complex⁶ of ruthenium(II), and this effect may be expected to become even more important in ruthenium(III) complexes of the $C(=O)-C(=NOH)$ function. The free-ligand ν_{NO} (1010 cm^{-1}) is shifted to much higher frequencies in the complexes, and this again is in line with the proposed ring resonance.

Magnetic Properties. Room-temperature magnetic susceptibility data agree with the low-spin (t_{2g}^3) $S = 1/2$ ground state. The strict symmetry of **1** is at best C_{2v} . That the effective symmetry of the ground electronic state is more is evident from the EPR spectra which have axial symmetry with well-defined g_{\parallel} and g_{\perp} both in the microcrystalline state (room

(1) Chakravarty, A. R.; Chakravorty, A. *Inorg. Nucl. Chem. Lett.* **1979**, *15*, 307.

(2) Vogel, A. I. "Practical Organic Chemistry", 3rd ed.; ELBS and Longman Group Ltd.: 1965; Chapter 4, p 720.

(3) Sawyer, D. T.; Roberts, J. L., Jr. "Experimental Electrochemistry for Chemists"; Wiley: New York, 1974; p 212.

(4) Chakravorty, A. *Coord. Chem. Rev.* **1974**, *1*, 1.

(5) Thornback, J. R.; Wilkinson, G. *J. Chem. Soc., Dalton Trans.* **1978**, 110.

(6) Bremard, C.; Muller, M.; Nowogrocki, G.; Sœur, S. *J. Chem. Soc., Dalton Trans.* **1977**, 2307.

Table II. Cyclic Voltammetric^a and Coulometric Data^b

compd	ν^c	E_{pc}	E_{pa}	ΔE_p	$E^{\circ'}_{298}$	Q_c^d	Q_e^e
RuCl ₂ (HB)(B) ^f	10–20	+0.428	+0.496	0.068	+0.462	1.23 ^g	-1.23 ^h +1.23 ⁱ
	50	+0.425	+0.500	0.075	+0.462		
RuCl ₂ (HB)(B) ^j	10	+0.330	+0.470	0.140			
	20	+0.320	+0.470	0.150			
	30	+0.300	+0.500	0.200			
RuBr ₂ (HB)(B) ^f	10–50	+0.470	+0.535	0.065	+0.503	1.23 ^k	-1.20, ^l +1.25 ^m

^a Meaning of all symbols as in the text; concentration $\approx 1 \times 10^{-3}$ M; 0.1 M TEAP as supporting electrolyte; potentials (in V) measured vs. SCE at 298 K at platinum electrode. ^b Controlled potential coulometry in acetonitrile; 0.1 M TEAP as supporting electrolyte. ^c Scan rate in mV s⁻¹. ^d Calculated coulomb. ^e Experimental coulomb. ^f In acetonitrile. ^g 7.9 mg RuCl₂(HB)(B). ^h Reduction at 0.0 V. ⁱ Oxidation at +0.8 V. ^j In dichloromethane. ^k 9.05 mg RuBr₂(HB)(B). ^l Reduction at 0.0 V. ^m Oxidation at +0.75 V.

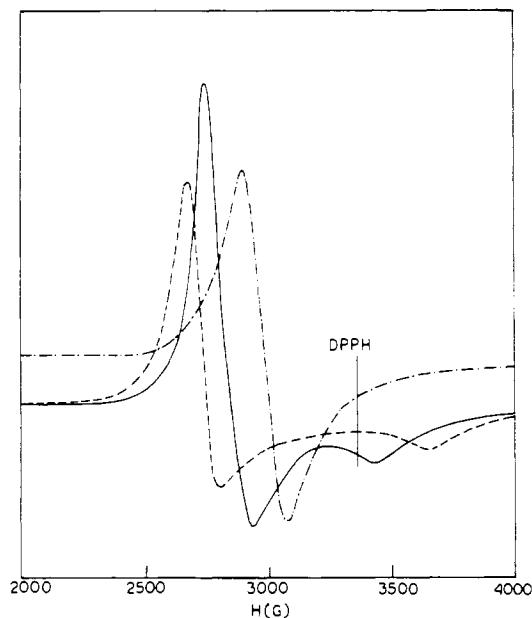


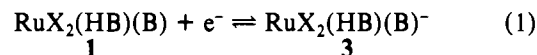
Figure 1. Room-temperature EPR spectrum of RuCl₂(HB)(B) (polycrystalline) (—), RuBr₂(HB)(B) (polycrystalline) (---), and RuCl₂(HB)(B) (benzene) (-.-.).

temperature) and in frozen benzene (123 K) (Table I). Representative spectra are displayed in Figure 1. Unlike many⁷ pseudooctahedral ruthenium(III) systems but like a few⁸ reported cases the observed *g*-tensor anisotropy in **1** is relatively small. No ligand hyperfine could be resolved in any of the spectra.

Cyclic Voltammetry and Coulometry. Complex **1** is electroactive at the platinum electrode. An electron-transfer process occurring near 0.5 V vs. SCE has been investigated by using cyclic voltammetry (CV). The process involves a single electron as proved conclusively by constant potential coulometry at 0.0 V (Table II). The reduced solution thus produced is quite stable particularly for X = Cl and can be quantitatively reoxidized to **1** by constant potential coulometry at +0.8 V (Table II). This cycle of coulometric oxidation and reduction can be repeated many times for X = Cl without apparent degradation of the complex. The CV of the reduced solution is the same as that of **1**. In the case of X = Br after one or two coulometric cycles, uncharacterized secondary reactions occur, producing a green solution.

In acetonitrile the separation (ΔE_p) between cathodic (E_{pc}) and anodic (E_{pa}) peak potentials lies within the range 65–70

mV at scan rates (ν) of 10–50 mV s⁻¹. The cathodic (i_{pc}) and anodic (i_{pa}) peak currents are equal in magnitude: $i_{pc}/i_{pa} \approx 1.0$. For a strictly reversible one-electron process at planar electrode, $\Delta E_p = 58$ mV. The observed process (eq 1) is thus



nearly but not exactly Nernstian. A part of the deviation of ΔE_p from the Nernstian value may however be due to reasons other than the lack of reversibility.⁹

The formal potential $E^{\circ'}_{298}$ calculated by using eq 2 follows

$$E^{\circ'}_{298} \approx 0.5(E_{pa} + E_{pc}) \quad (2)$$

the order $1 (X = \text{Br}) > 1 (X = \text{Cl})$. On the reasonable assumption that solvation energies of **1** and **3** do not change substantially in going from X = Cl to X = Br, the observed trend reflects the electron affinity order $1 (X = \text{Br}) > 1 (X = \text{Cl})$. Bromide stabilizes Ru(II) better than chloride does. The dc CV of **1** was also performed in dichloromethane solution (Table II). The electrode processes $1 \rightarrow 3$ and $3 \rightarrow 1$ are again observable, but ΔE_p is quite large, showing the presence of quasi-reversibility. Some ruthenium(III)–ruthenium(II) formal potential data in pseudooctahedral complexes containing the RuCl₂ moiety are as follows: *cis*-RuCl₂(NH₃)₄⁺ in H₂O, -0.346 V; *trans*-RuCl₂(NH₃)₄⁺ in H₂O, -0.426 V;¹⁰ *cis*-RuCl₂(bpy)₂⁺ in CH₂Cl₂, +0.30 V;¹¹ *trans*-RuCl₂(Hao)(ao) in CH₃CN, +0.503 V;¹² *trans*-RuCl₂(pap)₂ in CH₃CN, +0.925 V¹² (where bpy = α,α -bipyridine, Hao = phenylazobenzaldoxime, and pap = 2-phenylazopyridine).

Electronic Spectra. Solutions of **1** are reddish violet while those of **3** are deep blue. These colors are due to the presence of intense allowed—presumably of charge-transfer (CT) type—electronic transitions in the visible region (Table I). The ~ 535 -nm band in RuX₂(HB)(B) is tentatively assigned to LMCT and the ~ 640 -nm band in RuX₂(HB)(B)⁻ is assigned to MLCT where L = (HB)(B).

Conclusion. Ruthenium(III) complexes RuX₂(HB)(B) where X = Cl or Br have been synthesized. These have strong intramolecular hydrogen bonding, intrachelate resonance, and a *trans* RuX₂ configuration. The low spin ($S = 1/2$) t_{2g}^5 complexes display effective axial EPR spectra in polycrystalline state and in frozen benzene ($g_{\parallel} \approx 1.9$, $g_{\perp} \approx 2.5$). The systems exhibit a nearly reversible one-electron transfer at the platinum electrode; the $E^{\circ'}_{298}$ values are 0.46 and 0.50 V vs. SCE for X = Cl and Br, respectively, in acetonitrile. While RuX₂(HB)(B) displays an LMCT band at ~ 535 nm, RuX₂(HB)(B)⁻ has an MLCT transition at ~ 640 nm.

(7) Hudson, A.; Kennedy, M. J. *J. Chem. Soc. A* **1969**, 1116. Manoharan, P. T.; Mehrotra, P. K.; Taquikhan, M. M.; Andral, R. K. *Inorg. Chem.* **1973**, *12*, 2753.
(8) Sagüés, J. A. A.; Gillard, R. D.; Lancashire, R. J.; Williams, P. A. *J. Chem. Soc., Dalton Trans.* **1979**, 193. Murray, K. S.; Vanden Bergen, A. M.; West, B. O. *Aust. J. Chem.* **1978**, *31*, 203.

(9) Callhan, R. W.; Keene, F. R.; Meyer, T. J.; Salmon, D. J. *J. Am. Chem. Soc.* **1977**, *99*, 1064.
(10) Lim, H. S.; Barclay, D. J.; Anson, F. C. *Inorg. Chem.* **1972**, *11*, 1460.
(11) Johnson, E. C.; Sullivan, B. P.; Salmon, D. J.; Adeyemi, S. A.; Meyer, T. J. *Inorg. Chem.* **1978**, *17*, 2211.
(12) Chakravarty, A. R.; Goswami, S.; Chakravorty, A., to be submitted for publication.

Acknowledgment is made to the Department of Science and Technology, New Delhi, for financial support. Thanks are due to Dr. J. G. Mohanty of Hyderabad University for EPR spectra.

Registry No. 1 (X = Cl), 75400-19-0; 1 (X = Br), 75400-20-3; 3 (X = Cl), 75400-21-4; 3 (X = Br), 75400-22-5.

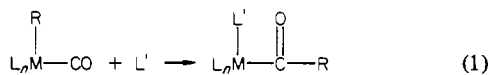
Contribution from the Department of Chemistry,
Northwestern University, Evanston, Illinois 60201

Acceleration of the Methyl Migration Reaction with Proton Acids

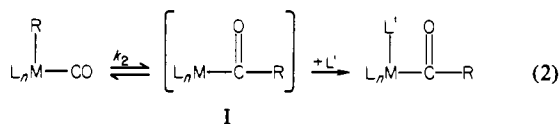
Susan Beda Butts, Thomas G. Richmond,
and Duward F. Shriver*

Received April 3, 1980

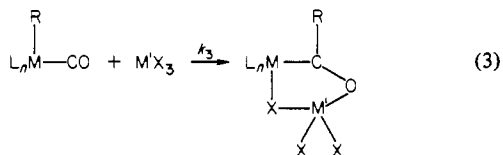
Our recent investigation of the influence of molecular Lewis acids on alkyl migration reactions in alkylmetal carbonyl complexes¹ and the known ion-pair promotion of alkyl migration² prompted us to study the effects of proton acids on this reaction. Many alkylmetal complexes are known to undergo an alkyl migration (CO insertion) reaction in the presence of added ligand (eq 1).³ These reactions are thought



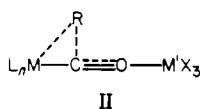
to proceed by way of a coordinatively unsaturated acyl intermediate (eq 2). We found that strong Lewis acids (e.g.,



AlCl₃, AlBr₃, BF₃) induce a rapid alkyl migration in a variety of complexes, even in the absence of added ligand, to produce novel ring adducts in which one halogen atom of the acid fills the open metal coordination site.¹ Since the rate of reaction with Lewis acid (reaction 3) is much more rapid than the



normal rate of formation of the intermediate I (i.e., $k_3 \gg k_2$), we propose that Lewis acid lowers the activation energy by coordination with the oxygen of the CO group which is undergoing reaction (II) and thus increases the overall rate of alkyl migration. The present investigation was prompted by the thought that proton acids might function in a manner similar to the Lewis acids and thereby increase the rate of reaction 1.



- (1) S. B. Butts, E. M. Holt, S. H. Strauss, N. W. Alcock, R. E. Stimson, and D. F. Shriver, *J. Am. Chem. Soc.*, **101**, 5864-5866 (1979).
- (2) J. P. Collman, R. G. Finke, J. N. Cawse, and J. I. Brauman, *J. Am. Chem. Soc.*, **100**, 4766 (1978).
- (3) A. Wojcicki, *Adv. Organomet. Chem.*, **11**, 87-145 (1973); F. Calderazzo, *Angew. Chem., Int. Ed. Engl.*, **16**, 299-311 (1977).

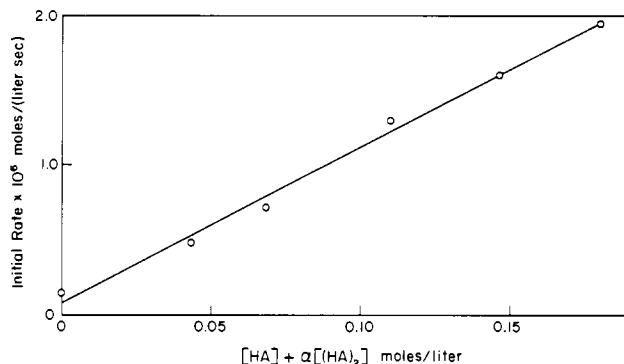


Figure 1. Initial rate of CO uptake vs. the concentration function $[HA] + \alpha[(HA)_2]$, where the two concentration terms apply to the monomer and dimer of CCl_2HCOOH . For all experiments $[Mn(C-H_3)(CO)_5] = 0.100 \pm 0.005 \text{ mol L}^{-1}$, $P_{CO} = 389 \pm 7 \text{ torr}$, $T = 20.0 \pm 0.1 \text{ }^\circ\text{C}$, and solvent = toluene.

Results and Discussion

As a model system we studied the reaction of $(CO)_5Mn(CH_3)$ and CO in the presence of a variety of proton acids (eq 4). Kinetic data for these experiments are summarized in

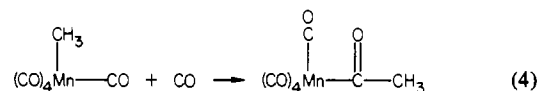


Table I. The observed enhancement of reaction rate caused by haloacetic acids increases with the strength of the acid. The strongest of these haloacetic acids, CF_3COOH , also caused significant $Mn-CH_3$ bond cleavage with resultant CH_4 formation. Thus, the greater rate enhancement caused by the stronger acid is offset by this detrimental cleavage. In the extreme case of the strong mineral acid HBr , the cleavage reaction is completely dominant. Formation of $BrMn(CO)_5$ and CH_4 occurs rapidly, and no alkyl migration is observed. Such acid cleavage reactions are well documented in the literature.⁵

The initial rate of reaction with CO was determined at 20 °C for several concentrations of CCl_2HCOOH .⁶ These data show a nonlinear dependence on nominal acid concentration, and a linear dependence of rate on acid monomer concentration, but, for the latter case, the extrapolated intercept at zero acid concentration indicates a negative rate, which is physically unacceptable. A satisfactory fit to all of the data, including the reaction in the absence of acid, is obtained by assuming that both the acid monomer and acid dimer accelerate the reaction according to eq 5. This equation contains initial rate =

$$\{k_u + k_1[HA] + k_2[(HA)_2]\}[Mn(CO)_5(CH_3)]P_{CO} \quad (5)$$

a term for the uncatalyzed reaction, k_u , the rate constant for the acid monomer path, k_1 , and the corresponding term for the acid dimer path, k_2 . Concentrations of the monomer and dimer were calculated by using the dimer formation constant determined by Steigman and Conkright ($K_D = 27.1 \text{ M}^{-1}$ in benzene at 25 °C; the ± 1.9 error in this value probably exceeds the difference between K_D at 25 °C and that at 20 °C).^{7,8} The

- (4) Z. Rappaport, "Handbook of Tables for Organic Compound Identification," CRC Press, Cleveland, Ohio, 1967.
- (5) (a) R. W. Johnson and R. G. Pearson, *Inorg. Chem.*, **10**, 2091-2095 (1971); (b) E. L. Muetterties and P. L. Watson, *J. Am. Chem. Soc.*, **98**, 4665-4667 (1976); (c) A. E. Stevens and J. L. Beauchamp, *ibid.*, **101**, 245-246 (1979); (d) P. L. Watson and R. G. Bergman, *ibid.*, **101**, 2055-2062 (1979); (e) A. Dawson, W. McFarlane, L. Pratt, and G. Wilkinson, *J. Chem. Soc.*, 3653-3666 (1962); (f) W. N. Rogers and M. C. Bard, *J. Organomet. Chem.*, **182**, C65-C68 (1979).
- (6) Dichloroacetic acid was studied because it caused the greatest rate enhancement without any detectable $Mn-CH_3$ bond cleavage.